Polymer Journal Vol. 1, No. 1, pp. 82–100 (1970)

# Temperature Dependence of Spherulitic Growth Rate of Isotactic Polystyrene.

## A Critical Comparison with the Kinetic theory of Surface Nucleation

Tadao SUZUKI* and André J. KOVACS

*CNRS—Centre de Recherches sur les Macromolécules, Strasbourg, France.*

(Received August 29, 1969)

ABSTRACT: Spherulitic growth rate of isotactic polystyrene was measured in a wide range of temperature using an original technique involving self-seeding and an accurate temperature control. The data are analysed according to the theoretical treatment of surface nucleation put forward by Hoffman *et al.* The free energy changes during crystallization are evaluated using three approximations, whereas the contribution of the mass transport to the growth rate was derived on the basis of the free volume, or the configurational free energy approach. The critical comparison of the theoretical predictions with the experimental data leads to conclusions concerning the practical use, the reliability and limitations of the present theroretical concepts.

KEY WORDS Spherulitic Growth Rate / Isotactic Polystyrene / Self-Seeding / Kinetic Theory / Mass Transport / Free volume / Configurational Free Energy /

Since isotactic polystyrene (*i*-PS) can be easily undercooled without appreciable crystallization, its crystallization kinetics and spherulitic growth rate can be conveniently investigated in a wide range of temperature, located between its melting point $T_m$ (~240°C) and its glass transition temperature $T_g$ (~90°C). For this reason many authors have already studied these phenomena[1–7] in *i*-PS, but in most cases the data were analysed on the basis of an oversimplified theoretical expression. This involves a constant activation energy for the mass transport across the liquid-crystal interface and an approximate relationship for the temperature dependence of the excess free energy $\Delta f_v$ of the liquid with respect to the crystal, controlling the nucleation process.

Recently these approximations were improved by Boon *et al.*[6–7] by introducing a WLF type equation[8] for the transport term and two different estimations of $\Delta f_v$, as suggested by Hoffman[9,10]. Similar improvements have been already used by Magill[11] and by Magill and Plazek[12] to analyse the spherulitic growth rate data of various compounds. In this latter work[12] an attempt has been made to compare the values of the transport parameters to those determined from shear creep investigations[13].

Using a similar approach we report here a new set of precise data on spherulitic growth rate of *i*-PS, measured between 112 and 200°C by an original technique involving self-seeding[14]. Our data and those reported previously by others[1–3,6] are compared critically with the theoretical expressions given by Hoffman[9,10]. Two approaches for evaluating the transport term were used, combined with three different approximations for $\Delta f_v$, one of them based on the enthalpy data of liquid, glassy and crystalline PS reported by Karasz *et al.*[15].

The optimal values of the different parameters involved were determined by a least mean square analysis of the data. The results are discussed in terms of the fundamental parameters controlling the segmental mobility in the liquid and the surface nucleation of chain folded crystalline lamellae. Further investigations on the same material, involving crystallization kinetics and self-seeding techniques will be reported in a subsequent paper[16].

* Present address: *Showa Denko Co. Tamagawa, Ohta-ku, Tokyo, Japan.*

## EXPERIMENTAL

### *Material*

All the experiments were performed on an *i*-PS sample received from the Laboratory of Prof. Natta*. This sample was purified by dissolution in boiling *o*-dichlorobenzene and filtration under nitrogen pressure. The filtered solution was then precipitated at room temperature in a large amount of methanol. The collected precipitate was dried in vacuo for several days.

The intrinsic viscosity of this sample in *o*-dichlorobenzene, at 25°C, was 3.57 $dl\ g^{-1}$, which corresponds, according to Krigbaum *et al.*[17], to an average molecular weight of $2.2\times10^6$.

The dried powder was then compression-molded (twice) at 260°C in the form of a 1 mm thick plate. The slightly yellow color of this sample indicated some thermal decomposition during the molding process. This has probably generated a small amount of low molecular weight products, which acted as a plasticizer and thus depressed both $T_m$ and $T_g$.

This sample has been used without further modification in the dilatometric investigations[16]. Its melting temperature, $T_m$*, as determined from self-seeding experiments[14], was 236°C and its glass transition, related to an experimental time-scale of 1 min, was $T_g$ (1 min) ~91°C.

The microscopic observations were performed on small chips cut from a film about 40 $\mu$ thick, molded at 260°C and inserted between two thin cover glasses.

### *Microscopy*

Four or six specimens sandwiched between cover glasses were placed into the slits (~0.5 mm) of a water-tight cylindrical aluminium block, which could be immersed in liquid thermostats[14]. After suitable thermal treatment to produce a convenient concentration of nuclei[16], generally by quenching to 100°C the specimens melted at 260°C, the block was finally immersed in a silicone oil bath maintained at the crystallization temperature $T_c$. The specimens were then successively removed from the block after increasing time periods $t$, and quenched to room temperature where the growth of spherulites is completely stopped.

As shown in Figure 1, the thermal treatment involving self-seeding[14,16] leads to specimens in which most of the spherulites have nearly identical diameter. This was measured under a polarizing microscope with a calibrated eyepiece micrometer. The average value of the radius $\bar{R}$ was determined from 20 to 40 individual measurements on the largest spherulites. In this group the individual measurements differed generally by less than 2%.

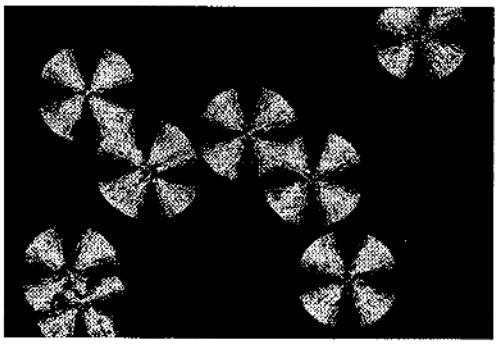

**Figure 1.** Self-seeding spherulites of *i*-PS grown at 175°C, seen between crossed nicols (150×).

The radial growth rate $G = d\bar{R}/dt$, which depends only on the temperature $T_c$, can be easily determined from the slope of the straight line obtained by plotting the average radius $\bar{R}$ *vs.* the time of residence $t$ of the specimen at $T_c$. A few examples of such plots are shown in Figure 2. The values of $G$, including duplicate experiments at slightly different $T_c$'s, are indicated in Table 1, as determined by the least mean square analysis of the data. One can see that the reproducibility is better than 1%.

The advantage of the method used is twofold. Firstly, the self-seeding ensures a practically simultaneous beginning of growth of the largest spherulites. Secondly, the crystallization temperature can be easily maintained constant for a long period (*e.g.* Figure 2, $T_c = 112$°C), which is very convenient for measuring slow growth.

The temperature of the silicone oil baths was maintained constant within $\pm$ 0.02°C. However, for long residence times uncontrolled temperature changes of the order of $\pm$ 0.1°C could be observed overnight. Even so, it is believed that the experiments were carried out at much better controlled values of $T_c$ than the previous ones, which involve the use of a hot stage. The temperatures were measured with a calibrated Hewlett-

* We are indebted to Professor F. Danusso for making this sample available to us.

**Table I.** The numerical values of spherulitic growth rate, $T_c \cdot \Delta S_3$ and $\Delta f_3$ at various crystallization temperatures

| $T_c$ (°C) | $10^4 G$[a] (cm·hr$^{-1}$) | $T_c \cdot \Delta S_3$[b] (joule·g$^{-1}$) | $\Delta f_3$[b] (joule·cm$^{-3}$) |
|---|---|---|---|
| 200.52 | 6.596 | 73.67 | 7.17 |
| 200.42 | 6.757 | 73.64 | 7.18 |
| 195.06 | 9.106 | 71.90 | 8.08 |
| 190.03 | 11.49 | 70.26 | 8.90 |
| 184.42 | 13.48 | 68.40 | 9.82 |
| 184.18 | 12.86 | 68.31 | 9.87 |
| 179.92 | 14.18 | 66.89 | 10.55 |
| 179.81 | 14.21 | 66.85 | 10.57 |
| 179.70 | 14.33 | 66.82 | 10.59 |
| 176.55 | 14.44 | 65.74 | 11.09 |
| 172.15 | 13.67 | 64.24 | 11.79 |
| 172.15 | 13.84 | 〃 | 〃 |
| 164.91 | 12.00 | 61.75 | 12.92 |
| 159.22 | 9.115 | 59.77 | 13.79 |
| 154.59 | 7.427 | 58.13 | 14.49 |
| 150.26 | 5.458 | 56.60 | 15.13 |
| 141.04 | 2.528 | 53.28 | 16.47 |
| 129.70 | 0.5429 | 49.14 | 18.06 |
| 119.62 | 0.0926 | 45.41 | 19.40 |
| 116.07 | 0.0430 | 44.08 | 19.86 |
| 112.01 | 0.0160 | 42.55 | 20.37 |

[a] As determined from least mean squares (Figure 2).
[b] cf. Eqs. 18 and 19 with $\Delta H_f = 86.3$ joule·g$^{-1}$ (91,100 joule·cm$^{-3}$). Obviously the decimals are beyond experimental accuracy. This precision is needed, however, for the numerical analysis of the data.

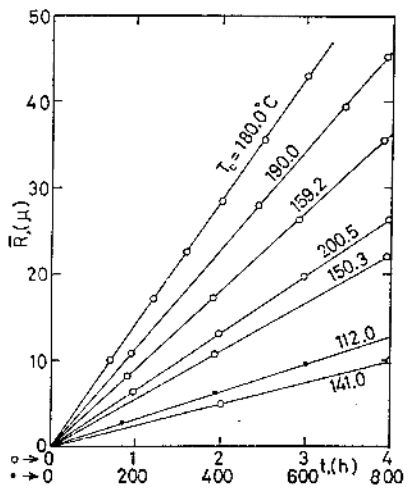


**Figure 2.** Average radius $\bar{R}$ (in $\mu$) *vs.* crystallization time in hours.

Packard quartz thermometer, the accuracy of which is better than $\pm$ 0.02°C.

The sandwiched specimens could be used after several cycles of melting and recrystallization. However, when the film was held for several hours above 180°C some thermal degradation occurred, starting at the edges in contact with the air. It has been noted that the growth rate is quite sensitive to degradation which results in an appreciable increase of the value of $G$. In fact, in such partially degraded films the spherulites grown near the edge may be twice as large as those located in the central part of the specimen. Of course these specimens were discarded. For the same reason we do not report here growth rates above 200°C; such data should be considered with caution. The isothermal increase of $G$ in the degraded samples should be attributed to the increase of the mass transport rate (*i.e.* molecular mobility) at the liquid-crystal interface, since the free energy difference $\Delta f_v$, remains practically unchanged.

*Results*

The experimental data are summarized in Figure 3, which shows the thermal variation of log $G$ measured at 17 temperatures, ranging from 112 to 200°C. Owing to the excellent reproducibility, duplicate measurements of the values of $G$, listed in Table I, were averaged in this plot; in fact the size of the circles is larger than the experimental scatter.

As already reported in earlier works[1-3,6] $G$ passes through a maximum in the range of 175~180°C. Figure 3 shows also the values of $G$ reported by Boon *et al.*[6a] which are reasonably close to our data. Comparison with other works[1,2] will be illustrated on a further graph (Figure 7).

The solid line represents one of the theoretical curves calculated with the optimal values of the free volume parameters (Table II), while using the first approximation for $\Delta f_v$ (Eq. 3), which will be discussed later. This curve does not differ appreciably from those involving better estimations of $\Delta f_v$, but it will be shown that the difference is significant if the configurational free energy[18] is considered rather than free volume[19] for evaluating the transport term.

Although the theoretical curve involving this

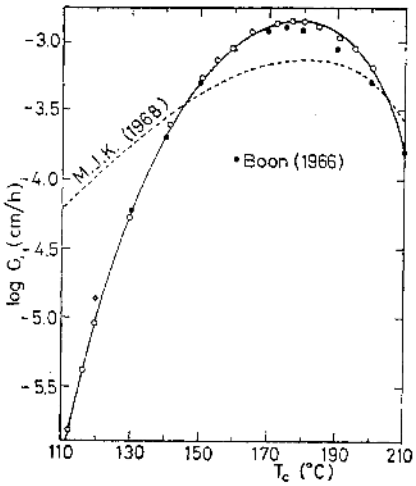


**Figure 3.** Spherulitic growth rate $G$ (in cm/hr) *vs.* crystallization temperature $T_c$ (in °C), open circles, this work; black points: data of Boon[6,7]. Solid line: theoretical curve based on the first approximation of $\Delta f_v$ and on the free volume approach. Broken line: theoretical curve proposed by Mandelkern *et al.*[4]

latter approach fits quite well the experimental values of $G$, in particular the agreement is much better than in any previous work[1,4,6], some systematic deviations may be noticed on both sides of the maximum (Figure 3), the magnitude of which (~4%) is about twice as great as the estimated accuracy of the experimental data (~2%).

## THEORETICAL

### *Surface Nucleation*

The characteristic features of the log $G$ *vs.* $T_c$ plot (Figure 3) suggest that the growth of spherulites obeys the general scheme of the Turnbull-Fischer[20] nucleation theory, which may be expressed as

$$G = G \exp\left(-\frac{\Delta F^*}{kT}\right) \cdot \exp\left(-\frac{\Delta \Phi^*}{kT}\right) \qquad (1)$$

Here, $G_0$ is a preexponential factor which is generally assumed temperature independent (or proportional to $T$). The first exponential factor: $\exp(-\Delta F^*/kT)$, the transport term, is the probability that in the local transport process a chain segment of critical length will reach the surface of the crystal. The second exponential factor: $\exp(-\Delta \Phi^*/kT)$, the nucleation term, represents the probability that the surface nucleus will reach a critical size. Accordingly $\Delta F^*$ is the free energy of activation for the transport process and $\Delta \Phi^*$ is the work required to form a stable nucleus of critical size, $k$ being the Boltzmann constant.

For the present purposes it will be assumed that the spherulitic growth proceeds through deposition of consecutive molecular layers of constant thickness $b_0$, the magnitude of which is related to the lattice spacing normal to the growth face[9,10]. Then according to the theoretical treatment of coherent surface nucleation in chain folded polymers (of high molecular weight) given by Lauritzen and Hoffman[21], $\Delta \Phi^*$ may be expressed to a good approximation[10] by

$$\Delta \Phi^* = \frac{4 b_0 \sigma \cdot \sigma_e}{\Delta f_v} \qquad (2)$$

where $\sigma$ and $\sigma_e$ are the work required to create 1 cm$^2$ of lateral and chain folded surface respectively, and $\Delta f_v$ the Gibbs' free energy difference between the supercooled liquid and the crystal (at the same $T$, per cm$^3$ of the crystal).

Assuming that $G_0$ is temperature-independent, one can evaluate the two exponential factors in Eq. 1 (essentially $\Delta F^*$ and $\Delta f_v$) in different ways.

### *First Approximations*

For the transport term the simplest approximation involves Eyring's rate theory[22] according to which the activation energy, $\Delta F^* = E$, is temperature-independent.

For the nucleation term (Eq. 2), $\Delta f_v = \Delta H - T\Delta S$, may be approximated by[10]

$$\Delta f_1 = \Delta H_f \frac{T_m - T}{T_m} = \Delta H_f \frac{\Delta T}{T_m} \qquad (3)$$

in which $\Delta H_f$ is the heat of fusion (per unit volume), $T_m$ the equilibrium melting temperature and $\Delta T = T_m - T$ the degree of supercooling. This first approximation of $\Delta f_v$ involves implicitly that $\Delta H$ and $\Delta S$ are both temperature-independent and equal to the heat ($\Delta H_f$) and the entropy of fusion ($\Delta S_f = \Delta H_f / T_m$) at $T_m$, where of course $\Delta f_v = 0$.

One can thus write (Eqs. 1–3)

$$\ln G = \ln G_0 - \frac{E}{RT} - \frac{4 b_0 \sigma \cdot \sigma_e T_m}{\Delta H_f \cdot \Delta T \cdot kT} \qquad (4)$$

where $R$ is the gas constant, and $E$ the molar

activation energy.

According to the different assumptions involved, this expression may be considered as a valuable approximation only if the investigations are limited to a rather narrow range of $T$ just below melting point, which is not the case for *i*-PS. In spite of this several authors[1,4] tried to apply Eq. 4 to the experimental data obtained with this polymer. The result is shown in Figure 3 by the broken line, which was calculated using Eq. 4 with the following parameters, given by Mandelkern *et al.*[4]

$$\left.\begin{aligned} E &= 20.2 \text{ kcal/mol} \\ K &= \frac{4b_0\sigma\cdot\sigma_e}{k\Delta H_f} = 263 \text{ deg} \\ T_m &= 527.2^\circ\text{K} \end{aligned}\right\} \qquad (4a)$$

whereas for $G_0$ we adopted the "universal" value ($\simeq 2.6\times10^8$ cm/hr) proposed by these authors.

It is obvious that Eq. 4 does not fit at all the experimental data represented in Figure 3. The fit is not better with the other data[1-3] even if the value of $G_0$ is considered as adjustable rather than universal. Since the discrepancy increases in the low temperature range where the transport term is predominant (cf. Eq. 4), Figure 3 shows clearly that an Arrhenius type approximation for this term is quite unsatisfactory. It is well known, on the other hand, that such an approximation also fails to represent the temperature dependence of configurational mobility in supercooled liquids[8,23-25] as determined from the thermal variations of the viscoelastic parameters above $T_g$.

*Theoretical Expressions of the Segmental Jump Rate*

Since the WLF equation[8] leads to an accurate fit of the temperature dependence of the viscoelastic parameters between $T_g$ and $T_g + 100$, it seems reasonable to adopt a similar expression for evaluating the transport term in Eq. 1. This was first pointed out by Hoffman *et al.*[26,27] and applied successfully by several authors[7,11,12] for representing the temperature dependence of spherulitic growth rate.

In their original treatment Hoffman *et al.*[10,27] expressed $\Delta F^*$ by

$$\Delta F^* = \Delta F_{WLF} = \frac{C_1 T}{C_2 + T - T_g} \qquad (5)$$

in which $C_1$ and $C_2$ are constants, respectively equal to 4.12 kcal/mol** and 51.6 deg, which were derived from the "universal" WLF constants[8]. However, in practice the authors use this relationship with adjustable parameters[7,11,12].

The WLF equation was related by its authors[8] to an empirical free volume concept of Doolittle[28] which was further justified theoretically by Cohen and Turnbull[19], and reinterpreted more recently by Adam and Gibbs[18] on the basis of configurational free energy changes rather than free volume. It seems more convenient to introduce here these two theoretical approaches for evaluating the transport term in Eq. 1, since both lead directly to the probability, $P$, of the configurational changes in supercooled liquids involved in the expression of the Turnbull-Fischer nucleation theory[20] (Eq. 1).

(a) According to Cohen and Turnbull[19] in the self-diffusion process, the transition probability of a molecule (or a molecular segment) is determined essentially by the chance of finding an adjacent local free volume greater than $v^*$, to jump into. This may then be expressed as

$$P(v^*) = \exp\left(\frac{-\bar{\gamma}v^*}{v_f}\right) = \exp\left(\frac{-b}{f}\right) \qquad (6)$$

where $v_f$ is the average free volume associated with the jumping unit and $\bar{\gamma}$ an overlap factor, lying between 0.5 and 1. Thus the ratio

$$\frac{v_f}{\bar{\gamma}v^*} = \frac{v - v_0}{\bar{\gamma}v^*} = \frac{v - v_0}{bv_0} = \frac{f}{b} \qquad (7)$$

is proportional to the fractional free volume $f$ of the liquid, since the average size of $v^*$ should be comparable to the "occupied" volume $v_0$ of the flow unit, $b = \bar{\gamma}v^*/v_0$, being a numerical factor of the order of 1.

Since the reciprocal of $P(v^*)$ is proportional to the retardation time $\tau$ for configurational changes (or to the relaxation time of stress, or to the viscosity $\eta$ of the liquid), Eqs. 6 and 7 are equivalent to the popular Doolittle equation[28], which can be written for $\tau$ (or $\eta$) as

$$\ln \tau \text{ (or } \eta) = a + \frac{b}{f} \qquad (8)$$

** This energy should not be confused with the apparent activation energy derived from the WLF equation which is strongly temperature-dependent[8,23].

the constant $a$ being the limiting value of ln $\tau$ (or ln $\eta$) when $f$ approaches infinity.

(b) Similarly, but from a completely different molecular kinetic treatment, Adam and Gibbs[18] derive for the average transition probability of configurational rearrangements the following expression

$$P(T) = \bar{A} \exp\left(\frac{-C}{TS_c}\right) \tag{9}$$

in which $\bar{A}$ is a temperature-insensitive factor, $C$ an energy related to the potential barrier for hindered rotation of the monomer unit, and $S_c$ the configurational entropy of the equilibrium liquid (stable or metastable). According to the authors the latter may be expressed by the integral

$$S_c(T) = \int_{T_2}^{T} \Delta C_p T^{-1} \cdot dT \tag{9a}$$

where $T_2$ is a limiting temperature below which configurational changes can no longer occur, and $\Delta C_p$ the difference of heat capacity of the (equilibrium) liquid and the glass (at the same $T$). Note that, according to Eq. 9a, $S_c(T)$ includes the excess entropy due to the excess volume of the liquid with respect to the crystal. It can be shown[18] that Eq. 9 leads, as a first approximation, to the Doolittle (or WLF) equation if $\Delta C_p$ is assumed temperature-independent.

In the following we will substitute successively these two expressions (Eqs. 6 and 9) of the transition probability in Eq. 1, and compare the results with the experimental data(Figure 3). Before doing this, it is worthwhile to introduce other estimations of the excess free energy $\Delta f_v$, which are more realistic than the first approximation used in Eqs. 3 and 4.

## HIGHER ORDER APPROXIMATIONS OF THE EXCESS FREE ENERGY

In fact the discrepancy between the data and Eq. 4 (cf. Figure 3) may not be due to the inaccuracy of the transport term alone, but also to rather crude first approximation used for evaluating the thermal variation of $\Delta f_v$ (Eq. 3).

*Second Approximation: $\Delta C_p$ = Constant*

Instead of assuming $\Delta H = \Delta H_f$ as in Eq. 3, it seems more reasonable to suppose, as already proposed by Hoffmann[9], that $\Delta C_p$ (the difference of heat capacity of the supercooled liquid and the crystal) is temperature-independent.

Accordingly, one can write

$$\Delta H_2 = \int_{T_2'}^{T} \Delta C_p \cdot dT = \Delta C_p (T - T_2') = \Delta H_f \frac{T - T_2'}{T_m - T_2'} \tag{10}$$

since

$$\Delta H_f = \Delta C_p (T_m - T_2') \tag{10a}$$

where $T_2'$, as in Eq. 9, is the lower limiting temperature where $\Delta H_2$ vanishes.

Consequently the excess entropy of the liquid with respect to the crystal may be expressed by

$$\Delta S_2 = \int_{T_2}^{T} \left(\frac{\Delta C_p}{T}\right) dT = \Delta S_f - \Delta C_p \ln \frac{T_m}{T} \tag{11}$$

where $T_2$ is the limiting temperature below which $\Delta S_2$ is negative.

Eq. 11 can be rearranged as

$$\Delta S_2 = \frac{\Delta H_f}{T_m}\left[1 - \frac{T_m \ln \frac{T_m}{T}}{T_m - T_2'}\right] \tag{12}$$

since

$$\Delta S_f = \frac{\Delta H_f}{T_m} = \Delta C_p \frac{T_m - T_2'}{T_m} \tag{12a}$$

One can thus write for $\Delta f_v = \Delta H_2 - T\Delta S_2$:

$$\Delta f_2 = \frac{\Delta H_f}{T_m}\left[\frac{T_m T \ln \frac{T_m}{T} - T_2' \Delta T}{T_m - T_2'}\right] \tag{13}$$

Approximating ln $(T_m/T)$ by $2\Delta T/(T_m + T)$, neglecting higher order terms, one has

$$\Delta f_2 \approx \frac{\Delta H_f \cdot \Delta T}{T_m} \times \left[\frac{T}{T_m} + \left(\frac{\Delta T}{T_m + T}\right)\left(\frac{T}{T_m} - \frac{T_2'}{T_m - T_2'}\right)\right] \tag{13a}$$

The second term between the brackets may be neglected because the first factor, $\Delta T/(T_m + T)$ is small near $T_m$ and the second vanishes at

$$T = \frac{T_m T_2'}{T_m - T_2'} \tag{14}$$

a temperature usually close to $T_g$[9]. Thus one obtains finally

$$\Delta f_2 \approx \Delta H_f \cdot \Delta T \frac{T}{T_m^2} \qquad (15)$$

which differs only by the factor $(T/T_m)$ from the first approximation (Eq. 3). This expression of $\Delta f_v$, when substituted in Eq. 2, may be considered as leading to a better approximation of the nucleation term, since it was derived from a more plausible assumption ($\Delta C_p$ = constant) than the first approximation ($\Delta H_1 = \Delta H_f$).

*Third Approximation*: $d(\Delta C_p)/dT$ = *Constant*

The basic assumption involved in the second approximation ($\Delta C_p$ = constant) is contradicted by the experimental data of $C_p$ reported by Karasz *et al.*[15] These authors measured accurately the heat capacity of amorphours and semicrystalline *i*-PS in a wide range of temperature (from 200 to 520°K) and compared the values of $C_p$ to those obtained with an atactic PS sample. Their main results, which will be used here for the third estimation of $\Delta f_v$, may be summarized as follows:

(1) Above $T_g$, for the amorphous samples, both isotactic or atactic, $C_p$ is a linear function of $T$, $(dC_p/dT)_{liq}$ being $3.275 \times 10^{-3}$ joule·g$^{-1}$·deg$^{-2}$ *.

(2) Below $T_g$, the $C_p$ values of the atactic and isotactic samples are practically equal (at the same $T$) irrespective of the crystallinity of the latter. This means that $C_p$ (glass) $\approx C_p$ (crystal), and consequently that $\Delta S = S_c$ (cf. Eq. 9a).

(3) The temperature coefficient of $C_p$ below $T_g$ is constant between 250 and 345°K, but it has a greater value than above $T_g$, since $(dC_p/dT)$ (glass, or crystal) $= 4.408 \times 10^{-3}$ joule·g$^{-1}$·deg$^{-2}$ **.

Hence $\Delta C_p$ decreases when $T$ increases, and one has in the temperature range of interest ($T_g < T < T_m$)

$$\Delta C_p = \Delta C_p^0 + \gamma T \; ; \quad T \geq T_g \qquad (16)$$

where $\Delta C_p^0 = 0.7021$ joule·g$^{-1}$·deg$^{-1}$ is the difference between the heat capacities of the supercooled liquid and the glass (or the crystal) at 0°K, as determined from the linear extrapolation of $C_p$ (liq) and $C_p$ (glass), and $\gamma$ is the difference between the temperature coefficients of these two heat capacities, its value being equal to $-1.132 \times 10^{-3}$ joule·g$^{-1}$·deg$^{-2}$.

Then, according to the previous procedure (Eqs. 10 and 11) we have

$$\Delta H_3 = \Delta H_f - \int_T^{T_m} (\Delta C_p^0 + \gamma T) dT$$

$$= \Delta H_f - \Delta C_p^0 \Delta T - \frac{\gamma}{2} \Delta T (T_m + T) \qquad (17)$$

and consequently

$$\Delta S_3 = \frac{\Delta H_f}{T_m} - \Delta C_p^0 \ln \frac{T_m}{T} - \gamma \Delta T \qquad (18)$$

Combining Eq. 17 and 18, $\Delta f_v$ can be expressed by

$$\Delta f_3 = \frac{\Delta H_f \cdot \Delta T}{T_m} - \Delta T \left( \Delta C_p^0 + \frac{\gamma \cdot \Delta T}{2} \right) + \Delta C_p^0 T \ln \frac{T_m}{T} \qquad (19)$$

if Eq. 16 holds. The parameters involved in these last three equations may be determined from direct measurements of the thermal properties of the polymer without invoking any extra assumption.

Eqs. 17 and 18 permit the calculation of the limiting temperatures $T_2$ and $T_2'$ (cf. Eqs. 9–11) where $\Delta H$ and $\Delta S$ respectively vanish. Adopting for $\Delta H_f$, 86.3 joule·g$^{-1}$, reported by Danusso and Moraglio[29], and with the above values of $\Delta C_p^0$, $\gamma$ and $T_m = 515.2$ K, this calculation leads to

$$\left.\begin{aligned} T_2 &= 276°\text{K} = 2.8°\text{C} \\ T_2' &= 216.4°\text{K} = -56.8°\text{C} \end{aligned}\right\} \qquad (20)$$

As already pointed out by Karasz *et al.*[15] $T_2$ and $T_2'$ have quite different values***. It is interesting to note, however, that following the suggestion of Hoffman[9] one should have (Eq. 14)

$$T_g \approx \frac{T_m T_2'}{T_m - T_2'} \qquad (21)$$

* Slope determined by least mean squares from 8 values of $C_p$ ($393 \leq T \leq 475$°K) of the atactic sample, and 6 values of $C_p$ of the molten isotactic sample ($T \geq 512$°K).

** As determined by least mean squares from 10 values of $C_p$ of the atactic sample ($250 < T < 345$°K) and from 5 values of the isotactic sample ($304 < T < 340$°K).

*** The values given here (Eq. 20) are slightly different from those reported by Karasz *et al.*[15] which are respectively equal to 280 and 237°K. This is due to a different estimation procedure of $\Delta H$ used by these authors.

This leads, with $T_g = 364°K$[16], to $T_2' = 213°K$, which is close to the value given above (Eq. 20). According to Eq. 10a this limiting temperature is compatible with a value of $\Delta C_p = \Delta H_f/(T_m - T_2') = 0.2856$ joule·g$^{-1}$·deg$^{-1}$ which is equal to that calculated from Eq. 16 at $T = 94.7°C$, a temperature only slightly higher than $T_g$[16]. Conversely, by calculating $\Delta C_p$ at $T_g$ from Eq. 16, ($\approx 0.309$ joule·g$^{-1}$·deg$^{-1}$), the corresponding value of $T_2'$, derived from Eq. 10a, is 236°K and virtually coincides* with that given by Karasz *et al.*[15].

In order to compare the different estimations of $\Delta H$, and $\Delta f_v$, we have plotted them in Figures 4 and 5, related to the unit volume of the crystalline phase, while adopting for the specific volume of the crystal: $v_c = 0.900 + 2.1 \times 10^{-4}$ $(T - 293)$ in cm$^3$·g$^{-1}$ [6,16]. Therefore,

$\Delta H_1 = \Delta H_f = 91.1$ joule·cm$^{-3}$ represents the first approximation (Eq. 3).

$\Delta H_2$ corresponds to the second approximation (Eq. 10) with $\Delta C_p$ = constant, while adopting for $T_2' = 213°K$, derived from Eq. 21, and indicated as $T_0$ in Figure 4.

$\Delta H_3$ was calculated from Eq. 17, using the values of $\Delta C_p^0$, $\gamma$, $\Delta H_f$ and $T_m$ given above, determined directly from the experimental data[15,29]. Figure 4 shows that this evaluation is intermediate between $\Delta H_1$ and $\Delta H_2$.

Similar plots may be obtained for the excess entropy $\Delta S$ by using Eqs. 3, 12 and 18. Figure 4 shows only the product $T\Delta S_3$ (determined from Eq. 18, using the same values of $T_m$ and $\Delta H_f$ as above), which may be identified in the case of *i*-PS with the configurational free energy $TS_c$ (Eq. 9), the fundamental rate controlling parameter in the Adam-Gibbs[18] treatment.

Although the differences between the three $\Delta H$ (or $\Delta S$) functions are quite important, the thermal variations of the excess free energy $\Delta f_v = \Delta H - T\Delta S$ is much less sensitive to the particular assumption used for estimating $\Delta H$, as shown in Figure 5. In fact, the third estimation of $\Delta f_v$ (Eq. 19) leads to an expression in which the principal term is precisely the first approximation (Eq. 3). Therefore, in the temperature range of interest, $\Delta f_3$ (listed in Table I) is nearer to $\Delta f_1$ than to $\Delta f_2$ (Figure 5). Nevertheless, the

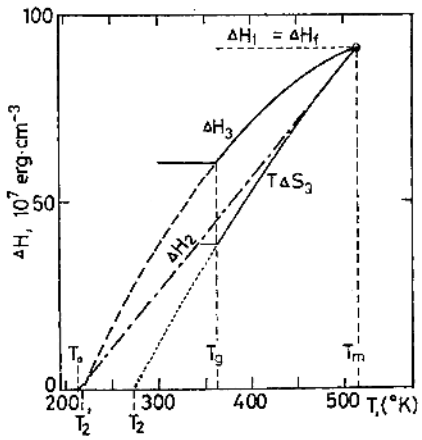


**Figure 4.** Temperature dependence of the excess enthalpy $\Delta H$ of the liquid with respect to the crystalline phase, according to three different approximations.

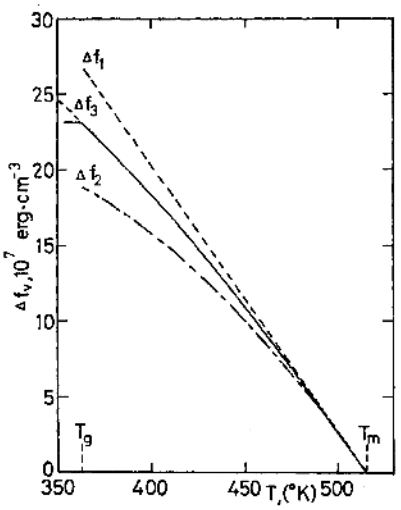


**Figure 5.** Temperature dependence of the excess free energy $\Delta f_v$ of the liquid with respect to the crystalline phase, according to three different approximations.

ratio $\Delta f_2/\Delta f_1 = T/T_m$ (Eqs. 3 and 15) is only slightly smaller than 1.

One can so expect that by substituting these three $\Delta f_v$ functions in Eq. 2, the final result will be also rather insensitive to the particular assumption involved. In a certain way this justifies—*a posteriori*—the popular first approximation (Eq. 3) used by most of the authors for representing the temperature dependence of spherulitic

* See footnote on page 88.

growth rate in polymers, even if the investigations were extended far below $T_m$. Thus the major part of the discrepancy shown in Figure 3 (broken line) should be attributed to the failure of the Arrhenius type approximation for the transport term (Eq. 4). In the following this latter will be estimated according to the two theoretical approaches given above (Eqs. 6 and 9).

## THE FREE VOLUME APPROACH

The theory will be tested first by using the free volume approach for the transport term associated with the three different estimations of $\Delta f_v$ (Figure 5). For doing this it is convenient to transform the expressions of the transition probability (Eq. 6) given by Cohen and Turnbull[19] in the following way.

Since the temperature dependence of $P(v^*)$ is related to that of the actual volume $v$ of the liquid (Eq. 7) one can reasonably assume that the fractional free volume $f$, is a linear function of $T$, provided $v$ varies linearly with $T$. Accordingly, adopting $T_g$ as a reference temperature, one has

$$f = f_g + \alpha_f (T - T_g) \geq 0 \qquad (22)$$

in which $f_g$ is the value of $f$ at $T_g$ and $\alpha_f = df/dT$ the temperature coefficient of the fractional free volume which is equal to the difference of the thermal expansion $\alpha$ of the liquid and that of $v_0$, *i.e.* $(1/v_0)dv_0/dT = \alpha_0$. This latter should be equal to (or less than) the thermal expansion $\alpha_g$ of the glass or $\alpha_c$ of the crystal[23,25] which are practically identical in the case of *i*-PS[16].

On the other hand, Eq. 22 shows that below a critical temperature

$$T_\infty = T_g - \frac{f_g}{\alpha_f} \qquad (23)$$

where $f = 0$, the transition probability is zero (Eq. 6) and consequently the viscosity and the retardation times for configurational changes (Eq. 8) reach an infinite value, provided that Eq. 22 holds in the whole temperature range where $f \geq 0$, *i.e.* that $v$ is a linear function of $T$. However, since $\alpha$ is rapidly decreasing below the glass transition, in practice Eq. 22 can be applied only above $T_g$, which is the case envisaged here. Thus the values of $f < f_g$ are related to the linearly extrapolated values of $v$ below $T_g$, *i.e.* to the equilibrium glass.

Consequently, the physical significance of the temperature $T_\infty$ (Eq. 23) is similar to that of $T_2$ or $T_2'$. At these critical temperatures the (extrapolated) thermodynamic parameters of the supercooled liquid reach a minimum value which characterize a fundamental stage (comparable to the crystal) in which configurational changes can no longer occur.

In practice, however, such a state cannot be obtained, since below the glass transition range the time required for reaching the configurational equilibrium becomes much longer than the usual experimental time scale[23,25].

On the other hand, since $T_2$, $T_2'$ and $T_\infty$ have different values, the actual problem is to decide which of these three temperatures is really the critical one, *i.e.* which of the thermodynamic excess parameters $\Delta S$, $\Delta H$ or $v_f$ controls effectively the molecular mobility in liquids[25,30], although the theories based on free volume[19] or on configurational free energy[18] lead formally to similar results above $T_g$.

By eliminating $T_g$ and $f_g$ in Eq. 22, *i.e.* by referring to $T_\infty$ (eq. 23), one can cast the expression of the reduced fractional free volume ($f/b$) in a more convenient form, since

$$\frac{b}{f} = \frac{b}{\alpha_f (T - T_\infty)} = \frac{B}{T - T_\infty} \qquad (24)$$

where $B = b/\alpha_f$ is a temperature-independent constant provided that $f$ varies linearly with $T$, *i.e.* above $T_g$.

This expression of $b/f$ transforms the Doolittle equation (Eq. 8) into a form given by Vogel[31] which was widely used for representing the temperature dependence of the viscosity of supercooled liquids (above $T_g$). Furthermore the ratios of viscosities or relaxation times at $T$ and $T_g$ may be then expressed by the popular WLF equation[8].

Finally, by identifying the transition probability $P(v^*)$, given by Eq. 6, with $\exp(-\Delta F^*/kT)$ in Eq. 1, one has $\Delta F^*/kT = B(T - T_\infty)^{-1}$. If this is compared to Eq. 5, one obtains

$$\left.\begin{aligned} B &= \frac{C_1}{R} = \frac{b}{\alpha_f} \\ C_2 &= T_g - T_\infty = \frac{f_g}{\alpha_f} \end{aligned}\right\} \qquad (25)$$

These relationships permit the conversion of the free volume parameters ($f_g$, $\alpha_f$) into the Vogel

($B$, $T_\infty$) or the WLF ($C_1$, $C_2$) parameters and *vice versa*.

*Test of the Free Volume Theory*

By substituting $B(T-T_\infty)^{-1}$ for $\Delta F^*/kT$ in Eq. 1 one can write for the spherulitic growth rate

$$\log G = \log G_0 - \frac{B}{2.303}(T-T_\infty)^{-1} - \frac{K}{2.303}\Delta H_f(\Delta f_v T)^{-1} \tag{26}$$

where the factor $K$, expressed by (cf. Eq. 2)

$$K = 4b_0\frac{\sigma\cdot\sigma_e}{k\cdot\Delta H_f} \tag{27}$$

contains all the parameters controlling the surface nucleation which are supposed to be temperature-independent, provided that $\Delta H_f$ as $\Delta f_v$, is estimated per unit volume of the crystal.

By substituting successively the three different estimations of $\Delta f_v$ (Eqs. 3, 15, and 19), one can compute the optimal values of the four adjustable parameters $G_0$, $K$, $B$, and $T_\infty$ which minimize the differences between the calculated and the experimentally measured values of $G$ (Table I, Figure 3).

Consequently the three expressions to be compared to the experimental data may be written as follows

(1) $$\log G = \log G_{0,1} - \frac{B_1/2.303}{T-T_{\infty,1}} - \frac{(K_1/2.303)T_m}{T\cdot\Delta T} \tag{28}$$

is the first approximation, already used by several authors[11,12] for analysing growth rate data.

According to the second approximation[9] one should have (Eq. 15)

(2) $$\log G = \log G_{0,2} - \frac{B_2/2.303}{T-T_{\infty,2}} - \frac{(K_2/2.303)T_m^{\,2}}{T^2\cdot\Delta T} \tag{29}$$

Finally, by using the values of $\Delta f_3$, listed in Table I, which were calculated from Eq. 19 using the numerical values of $\Delta H_f$, $T_m$, $\Delta C_p^{\,0}$ and $\gamma$ (Eq. 16) given above, the third approximation may be written as

(3) $$\log G = \log G_{0,3} - \frac{B_3/2.303}{T-T_{\infty,3}} - \frac{(K_3/2.303)\Delta H_f}{T\cdot\Delta f_3}. \tag{30}$$

In all these three equations $K$ is defined by Eq. 27, but it has different values, according to the approximation used for $\Delta f_v$.

The optimal values of the four adjustable parameters ($G_0$, $B$, $T_\infty$ and $K$) figuring in Eqs. 28–30 were determined from a least mean square analysis of the experimental data, while using all the 21 values of $G$ listed in Table I.

In each case, after selecting a reasonable value of $B$, successive values of $T_\infty$ (located in the expected range of $T$, and differing by 0.1~0.5°C) were substituted into the above equations in order to calculate $G_0$ and $K$ and the standard error* $\sigma(K)$. This error had generally a rather sharp minimum for an optimal value of $T_\infty$ (which could be specified within a tenth of a degree) associated with the selected value of $B$. (Two such particular curves of $\sigma(K_1)/K_1$ are shown in Figure 6 by dotted lines). The same procedure is then repeated for other values of $B$, selected in order to decrease the minimum of $\sigma(K)$, associated with the corresponding optimal values of $T_\infty$. Alternatively, since $B$ and $T_\infty$ contribute symmetrically to the transport term, one can also select first a value of $T_\infty$ and look for the optimal value of $B$ which minimizes $\sigma(K)$.

It has been found that the trial values of $B$ and the associated optimal values of $T_\infty$ (or *vice versa*) minimizing $\sigma(K)$ are related almost linearly, as shown in Figure 6, the slope $(dB/dT_\infty)_{opt}$ ($\approx 25$) being practically independent on the approximation used for estimating $\Delta f_v$, at least in the temperature range of interest.

Consequently one can plot the minimum values of $\sigma(K)/K$ against the corresponding optimal values of $T_\infty$, which are associated with those of $B$ according to the almost linear relationship mentioned above (Figure 6). These minima of $\sigma(K)/K$ represented in Figure 6 for each of the three approximations of $\Delta f_v$, pass through a rather flat minimum, which corresponds to the best couple of optimal values of $T_\infty$ and $B$. Consequently, they define the "best" values of the two other parameters, $G_0$ and $K$, for the most accurate fit of the experimental data by Eqs. 28–30. These calculations were performed by an IBM 1130

* See the Appendix.

computer using a Fortran program.

As expected, Figure 6 shows that the best couple of values of $T_\infty$ and $B$ do not depend critically on the approximation used for $\Delta f_v$. The same holds also for the two other parameters, $G_0$ and $K$, listed in Table II, in which the free volume parameters corresponding to the best couple of $B$ and $T_\infty$ (Eq. 25) are also indicated. These values are related to a melting temperaure $T_m = 515.2°K$. In fact, the best values of the four parameters involved in Eqs. 28–30 are quite sensitive to $T_m$, since by increasing the melting point by 3 degrees, the variations of the best $G_0$, $B$, $T_\infty$ and $K$ are more important than those related to the different estimations of $\Delta f_v$ (Eqs. 28–30). This is shown in Table II, while using the first approximation of $\Delta f_v$ (Eq. 28) associated with a melting point $T_m = 518.2°K$. However, even in this case, the variations of the characteristic parameters are quite small, since the upper limit of the temperature range investigated is still more than 40°C below $T_m$.

Furthermore, Figure 6 shows also that the Arrhenius type approximation for the transport term (cf. Eq. 4) is quite unsatisfactory. In fact, this approximation is a limiting case of the Vogel equation (Eq. 24) if $T_\infty$ is equal to 0°K. Figure 6 shows clearly that this value of $T_\infty$ should lead to a quite large error $\sigma(K)$, since the best values are all located in the vicinity of 330°K (cf. Table II).

Finally, Figure 6 shows somewhat paradoxically that the first approximation of $\Delta f_v$ (Eq. 28) leads

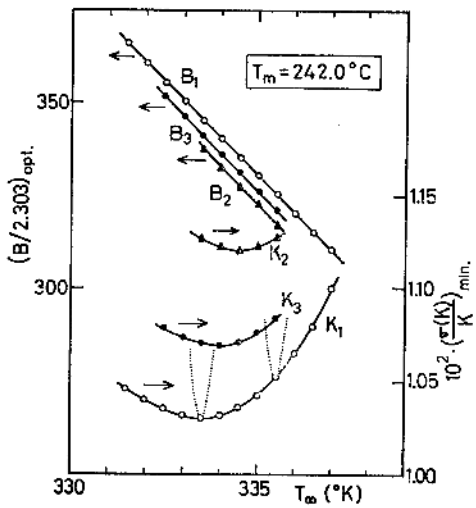


**Figure 6.** Variations of the optimal values of the Vogel parameter $B$ associated with that of $T_\infty$. Variations of the minimum relative error $\sigma(K)/K$ involved as a function of the optimal values of $T_\infty$.

**Table II.** Transport and nucleation parameters of growth rate of *i*-PS

| $T_m$ (°K) | Eq. | log $G_0$ (cm·hr$^{-1}$) | $B$/2.303 (deg) | $T_\infty$ (°K) | $K$/2.303 (deg) | $T_g$ (°C) | $T_g - T_\infty$ (°C) | $10^3\alpha_f/b$ (deg$^{-1}$) | $10^2 f_g/b$ | $b\alpha_f/f_g^2$ (deg$^{-1}$) |
|---|---|---|---|---|---|---|---|---|---|---|
| 515.2 | 28 | 1.8876 | 345.2 | 333.5 | 100.3 | 91.0 | 30.7 | 1.26 | 3.86 | 0.846 |
| | 29 | 2.0336 | 327.6 | 334.5 | 101.2 | 〃 | 29.7 | 1.32 | 3.94 | 0.851 |
| | 30 | 1.8889 | 333.6 | 334.2 | 100.7 | 〃 | 30.0 | 1.30 | 3.90 | 0.855 |
| | 31 | 6.856 | (462.4)[a] | (276.0)[b] | 143.4 | 〃 | 88.2 | — | — | — |
| 518.2 | 28 | 2.1733 | 363.7 | 332.0 | 114.2 | 〃 | 32.2 | 1.19 | 3.84 | 0.807 |
| 513.0 | 28[c] | 4.74 | 904 | 283 | 121.1 | 85 | 75.0 | 0.48 | 3.60 | 0.37 |
| | 29[d] | 6.66 | 904 | 312 | 204.6 | 〃 | 51.6 | 0.48 | 2.48 | 0.78 |
| 527.2 | 4[e] | 8.41 | 441.4 | 0 | 114.2 | 100 | 373.2 | 0.10 | 3.73 | (0.072) |
| $\tau$[f] | 8 | — | 320 | 342.6 | — | 97.0 | 27.6 | 1.36 | 3.75 | 0.96 |
| $\eta$[g] | 〃 | — | 837 | 312.3 | — | 100.0 | 60.9 | 0.52 | 3.16 | 0.52 |

[a] $C$/2.303, (cf. Eqs. 9 and 31) in joule·g$^{-1}$.
[b] Limiting Temperature $T_2$, cf. Eq. 20.
[c] Data in ref. 7a.
[d] Data in ref. 6b.
[e] Data reported by Mandelkern *et al.*[4], with $T_\infty = 0$; $B = E/R$ and $b\alpha_f/f_g^2 = E/R\,T_g^2$, (Figure 3, broken lines)
[f] Data of Plazek[39], atactic PS, $M_w = 46900$.
[g] Unpublished data of R. Suzuki and Kovacs[35], atactic PS fractions, $M_w > 40000$.

to a better fit than $\Delta f_3$ determined directly from the experimentally measured heat capacity data[15], whereas the second approximation (Eq. 29) leads to the less accurate fit. This again justifies *a posteriori* the use of the first approximation associated with the Vogel equation, for fitting growth rate data[11,12].

However, since the average minimum errors $\sigma(K)$ are small and quite close (Figure 6) one cannot assert that the first approximation is significantly better than the others. Moreover, the difference between the experimental and calculated values of $G$ varies systematically with $T$ but independently of the approximation used for $\Delta f_v$ (cf. Figure 8). This rather frustrating conclusion should be attributed to the small differences between the three estimations of $\Delta f_v$ (Figure 5) and to the fact that in the temperature range investigated the contribution of the nucleation term is generally smaller than that of the transport term. Thus the small systematic deviations, as shown in Figures 2 and 8 should be attributed to the inaccurate evaluation of the latter.

In Figure 7, we have plotted $\log G + B(T-T_\infty)^{-1}$ *vs.* $T_m/T\cdot\Delta T$, with $B = B_1 = 345.2°K$, $T_\infty = T_{\infty,1} = 333.5°K$, and $T_m = 515.2°K$, corresponding to the first approximation (Table II). This graph also includes some growth rate data obtained with *i*-PS by other authors[1,2,7]. It can be seen that with the exception of a few points all these data are reasonably well represented by Eq. 28 while using the best values of the transport parameters derived from the data reported in this work. However, owing to the vertical shift to superimpose different parallel straightlines, the values of $G_0$ are quite different. This may be attributed to the difference in molecular weight and tacticity of the samples. Similar features were already reported with other polymers[14].

The nucleation parameters, derived from the best values of $K$ (Eq. 27) listed in Table II, will be discussed later.

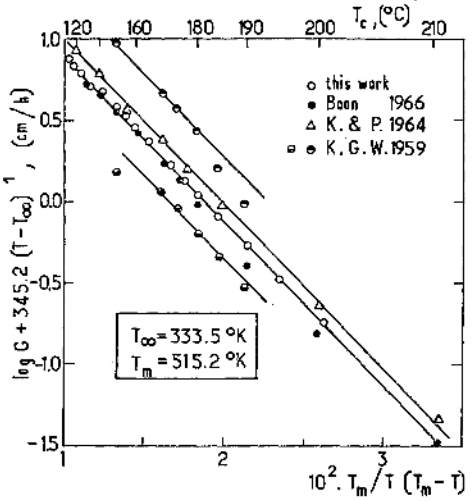


**Figure 7.** Plots of $\log G + B_1 (T-T_\infty)^{-1}$ *vs.* $T_m/T(T_m - T)$, derived fromthe experimental data reported by different authors[1,2,6], with $B_1 = 345.2°K$ and $T_m = 515.2°K$.

## THE CONFIGURATIONAL FREE ENERGY APPROACH

Instead of the Vogel equation related to the free volume concept, one can also introduce for the transport term (cf. Eq. 1) the transition probability given by Adam and Gibbs[18]. Since for *i*-PS the isothermal entropy difference between the glass and the crystal may be neglected[15], *i.e.* $\Delta S = S_c$, this leads, similarly to Eqs. 26, (cf. Eqs. 1, 2, and 9) to

$$\log G = \log G_0' - \frac{C/2.303}{T\Delta S} - \frac{(K'/2.303)\Delta H_f}{T(\Delta H - T\Delta S)} \tag{31}$$

$K'$ being defined by Eq. 27. The main difference between this equation and Eq. 26 derived from the free volume approach is that it contains only three adjustable constants ($C$, $K'$, and $G_0$) instead of four, since the parameter $T\Delta S$ controlling the transport process appears also in the nucleation term.

This permits, of course, a much simpler numerical analysis of the experimental data, since one can minimize the standard error $\sigma(K')$ using one set of reasonable values of $C$.

One can again substitute for $\Delta f_v$ the three approximations already used in the free volume approach. However, in contrast to the previous calculations, the final result will be quite sensitive to the approximation used, since the choice of $\Delta f_v$ necessarily involves the estimation of $T\Delta S$ which appears alone in the transport term of Eq. 31. Consequently, the first approximation of $\Delta f_v$ (Eq. 3) involving $\Delta S = S_c = \text{constant}$, should

be rejected *a priori*, since it reduces the Adam-Gibbs transition probability (Eq. 9) to an Arrhenius type equation (cf. Eq. 4 with $E/R = C/S_c$ = constant), which leads to a rather poor fit of the experimental data (cf. dotted lines in Figure 3).

The second approximation which involves $\Delta C_p$ = constant may be used. However, owing to the ambiguity of its derivation (Eqs. 13–15, only the third estimation of $\Delta f_v$ based on experimental data[15] will be considered here, since it does not involve any extra assumption.

Since in the original work of Adam and Gibbs[19] $TS_c$ was related to the unit mass of the material instead of unit volume, the calculation of the transport term was performed here by evaluating $T\Delta S_3$ in joule·g$^{-1}$ from Eq. 18, while $\Delta f_3$ was estimated as previously in joule·cm$^{-3}$ (cf. Table I). It was confirmed that the values of $C$ and $K'$ (Eq. 31) do not change appreciably if $T\cdot\Delta S_3$ is related to the unit volume.

The least mean square analysis of the data according to Eq. 31, and the third evaluation of $\Delta S$ and $\Delta f_v$, as mentioned, lead to the following best values of the parameters involved

$$\left.\begin{aligned} C/2.303 &= 462.4\ \text{joule}\cdot\text{g}^{-1} \\ K'/2.303 &= 143.4\ \text{deg} \\ \sigma(K')_{\min}/K' &= 0.0247 \\ \log G_0'(\text{cm/hr}) &= 6.856 \end{aligned}\right\} \quad (32)$$

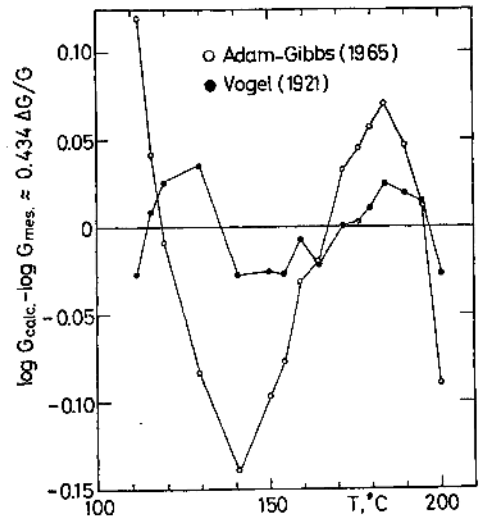


**Figure 8.** Thermal variation of the difference between the calculated and measured values of log $G$, obtained by estimating the transport term from the free volume (black points) and the configurational free energy (open circles) approaches.

while assuming, as previously, $\Delta H_f = 91.1$ joule·cm$^{-3}$ and $T_m = 515.2$°K. The value of $C$ may be transformed into 26.5 kcal/mol of monomer units, the magnitude of which is comparable to the activation energy $E$ reported by Mandelkern *et al.*[4] (cf. Eq. 4a) and Kenyon *et al.*[1] This value seems, however, too large to be associated with the flex energy barrier of C–C bonds, as originally suggested by Adam and Gibbs[18,24].

Furthermore, the values of the other parameters (Eq. 32) are much larger than those obtained from the free volume approach (Table II); in particular $G_0$ is greater by more than 4 orders of magnitude, and $\sigma(K')/K'$ is more than twice as great as for the free volume approach. This leads of course to a much poorer fit than Eqs. 28–30.

In Figure 8 we have plotted *vs.* $T_c$ the difference between the calculated and the measured values of log $G$, which is about half of the value of $(G_{calc} - G_{mes})/G_{mes} = \Delta G/G^*$.

It can be seen that in both cases there is a systematic variation of the deviation from the experimental data, although the free volume approach leads to a much closer fit than the Adam-Gibbs theory. As already mentioned, however, the former involves an additional parameter. Since in the low temperature range ($T < 145$°C) the deviations are of opposite sign it is obvious that the two evaluations of the transport term cannot be reconciled although $T\cdot\Delta S_3$ (Figure 4), like $f$ (Eq. 22), varies almost linearly with $T$. The major difference between the two approaches arises from the difference between the limiting temperatures $T_2$ and $T_\infty$ (cf. Eq. 20 and Table II) which is about 60°C. In fact at $T_\infty \approx 330$°K (Figure 6), below which according to the free volume approach configurational changes can no longer occur, the Adam-Gibbs theory provides considerable mobility, since the value of $T\cdot\Delta S_3$ is still a large fraction of the one obtained at 175°C, where the growth rate has its maximum (cf. Figure 4). Consequently, the only manner to force the Adam-Gibbs theory for a better fit of the data, is to introduce a higher limiting temperature for $T\Delta S$ (comparable to

* The vertical scale of this graph is too small to show any significant difference between the three sets of the calculated values of log $G$ based on the free volume approach (Eqs. 28–30).

$T_\infty$) than the one derived from the extrapolation of thermal properties of the material. In this case of course the two approaches become equivalent, with a small difference related to the slightly non-linear temperature dependence of $T \cdot \Delta S_3$ (Figure 4).

## DISCUSSION

*Transport Parameters*

It is interesting to compare the magnitude of the transport parameters derived from the above calculations to those obtained from the temperature dependence of the viscoelastic properties (viscosity $\eta$, or retardation times $\tau$). These latter values are listed in Table II, as derived from creep investigations on atactic PS samples of high molecular weight ($M_w > M_e \approx 40000$) while using the Doolittle or the Vogel equation (Eqs. 8 and 24). This table also shows the transport parameters used by Boon *et al.*[6b,7a] for interpreting their growth rate data, which were converted into the free volume parameters according to Eq. 25. Since these authors analysed their data on the basis of the WLF equation (Eq. 5) while using the "universal" values of the parameters[6b], or by changing one of them ($C_2 = T_g - T_\infty$)[7a] in order to obtain an acceptable fit, it is not surprising that their values are rather far from those obtained in this work, where both of the free volume parameters are assumed adjustable. Table 2 includes also the parameters proposed by Mandelkern *et al.*[4] which were already discussed (Eq. 4a; Figure 3).

By comparing the best transport parameters derived from the free volume approach to those obtained from the temperature dependence of $\eta$ or $\tau$, one can see that the values of $T_\infty$ are in rather good agreement, whereas those of $B/2.303$ (or $\alpha_f/b$; cf. Eq. 25) are quite close to the value deduced from the recoverable creep ($\tau$) investigations[18] (Table II). The discrepancy between the values of $B$ (or $\alpha_f/b$) derived from the temperature dependence of $\eta$ and $\tau$ may be attributed to the entanglement coupling of the chains which contributes differently to the recoverable creep than to the flow[32]. The relative agreement between the values of the transport parameters derived from $G$ and $\tau$ (Table II) may thus indicate that the "reeling in" of molecules during the crystal growth is comparable to their movement in a creep process.

However, the 1 to 2 ratio of the parameter $B$, or $\alpha_f/b$, obtained from $G$ and $\eta$, may be interpreted also on the basis of a more specific model directly related to the temperature dependence of the local free volume near the growing face. In fact, the latter may be about twice as large as in a volume element of the pure liquid phase, because the crystallization involves a volume shrinkage $\Delta v = (v_l - v_c)$ per g, the temperature coefficient of which $(\alpha - \alpha_c)$ is the same order of magnitude as $\Delta\alpha = \alpha - \alpha_g$, *i.e.* $\alpha_f$, according to the free volume concept ($\alpha$, $\alpha_c$, and $\alpha_g$ being the thermal expansion of the liquid, the crystal and the glass, respectively). In other words it may be conceived that the volume shrinkage contributes as much to the local free volume near the growing face of the crystal as the brownian motion in the pure liquid phase, the temperature coefficients of both processes being of the order of $\Delta\alpha$.

Similar conclusions may be drawn from the data reported by Magill and Plazek[12,13] on growth rate, viscosity and creep of Tri-$\alpha$-naphtylbenzene, analysed on the basis of the Vogel equations (Eqs. 24 and 28). Their results show that $\alpha_f/b$ (as determined from the reciprocal of the values of $B$, cf. Eq. 25) is more than twice as large when derived from the temperature dependence of the growth rate than from that of $\eta$ (or $\tau$). For this material, however, the value of $T_\infty$ determined from $G$ was about 100°C higher than that obtained from $\eta$ (or $\tau$)[12,13,33], whereas in the present case the difference of $T_\infty$ is only of the order of $\pm$ 10°C (cf. Table II).

In the last column of Table II we have listed the ratios $b\alpha_f/f_g^2$, derived from the free volume approach which measure the temperature coefficients $d \ln P(v^*)/dT$, (Eqs. 6 and 22), *i.e.* of molecular mobility at the reference temperature $T_g$. This ratio may also be obtained from the shift factor $a_T$ for superimposing the volume contraction isotherms[23,34] of the quenched glass along the log time axis. Such data reported in a subsequent paper[16] lead, for the same *i*-PS, to $b\alpha_f/f_g^2 = 0.81$ deg$^{-1}$, which is in gratifying agreement with the values obtained here from growth rate data and confirms the self-consistence of the free volume approach.

*Nucleation Parameters*

(a) It should be pointed out, that the values of the main nucleation parameter $K$ (Eq. 27), given in Table II, are independent of the adopted values of $\Delta H_f$[29], provided that the first, or the second approximation (Eq. 28 or 29) is used for estimating $\Delta f_v$. For the third approximation (Eq. 30 or 31), however, the value of $K_3$ or $K'$ depends slightly on the particular value of $\Delta H_f$, which enters as a factor only the principal term of $\Delta f_3$ (Eq. 19). Consequently the ratio $\Delta H_f/\Delta f_3$ appearing in the nucleation term of Eqs. 30 and 31 will not be modified much by changing $\Delta H_f$, since such a change will affect only the contribution of the corrective terms of $\Delta f_3$. If the data are analysed as above, i.e. leaving the transport and the nucleation parameters adjustable, a slight change of $K$ results in a small change of the "best" values of the transport parameters. If the Adam-Gibbs approach is used (Eq. 31) the modification of the value of $C$ is more important, since $T\cdot\Delta S_3$ (Eq. 18) depends also on the value of $\Delta H_f$. In particular the limiting temperature $T_2$ (cf. Figure 4) where $\Delta S_3$ vanishes, will change with $\Delta H_f$.

Table II shows that the magnitude of $K$ (or $\sigma\sigma_e$) does not depend critically either on the type of approach used for the evaluation of the transport term (Eqs. 4, 28–31), or on the values of the parameters involved, which vary in a wide range. Interestingly enough, even Eq. 4, as used by Mandelkern *et al.*[4], leads to an acceptable value of $K$.

On the other hand, the growth rate data of *i*-PS reported by others[1,3,7] lead to similar values of $K$, as shown in Figure 7, where the slope of the parallel straight lines is equal to $-K_1/2.303$. Moreover, the value of $K$ seems almost independent of the chemical composition of the polymer. In fact for the two polymers, polyethylene (PE) and polychlorotrifluoroethylene (PCTFE), whose growth rate data were the most thoroughly analyzed[10,36], thevalue of $K$ (respectively equal to 230 and 280 deg) is quite close to those reported here ($230 < K < 260$; cf. Table II) for *i*-PS. Similar analysis of growth rate data of isotactic Polybutene-1 (PB-1; forme II), derived from two sets of independent measurements on different samples, lead to $K = 290$[37] and 305 deg[14,38]. The $K$ values reported by Magill[11b] for Nylon 6 and 66, respectively equal to 295 and 205 deg, are also located in the same range.

This conclusion is similar to the one proposed recently by Mandelkern *et al.*[4], although these authors analysed the available growth rate data on the basis of Eq. 4, while assuming $T_m$ and $E$ to be adjustable and $K$ and $G_0$ to be "universal".

It should be pointed out however, that the nucleation parameter $K$ enters the above equations as an exponent. Therefore a small variation of its magnitude provokes a large change of the value of $G$, as portrayed in Figure 3, in which the two theoretical curves were calculated using two values of $K$ differing by less than 15 percent (cf. Table II). Consequently the thumbrule of the universality of the main nucleation parameter, as proposed by Mandelkern *et al.*[4] should be handled with caution. It may just show that the work required for chain folding[10].

$$q = 2A_0\sigma_e \tag{33}$$

where $A_0$ is the cross-section of the chain, does not depend critically on the chemical composition[27]. In fact, by assuming like Hoffman *et al.*[10,27] that

$$\sigma = \beta\cdot\Delta H_f\cdot b_0 \tag{34}$$

where $\beta$ is a numerical factor of the order 0.1 for chain like molecules, one can write approximately (Eq. 27)

$$K = \frac{4b_0\sigma\cdot\sigma_e}{k\Delta H_f} \approx \frac{4\beta b_0^2\cdot\sigma_e}{k} \approx \frac{2\beta q}{k} \tag{35}$$

since $b_0^2$ and $A_0$ are of comparable magnitude.

(b) The values of $K$ given in Table II lead directly to the product $\sigma\cdot\sigma_e$ of the surface free-energies (cf. Eq. 27) if $\Delta H_f$ and $b_0$ are known from independent measurements. According to the rhombohedral unit cell dimensions given by Natta *et al.*[40] ($a = b = 21.9$ Å, $c = 6.65$ Å, $\gamma = 2\pi/3$; at 20°C) the average cross section $A_0$ of the *i*-PS chain in the crystal amounts, at 160°C, to $70.5\times 10^{-16}$ cm$^2$. Thus $b_0$ may be approximated as above by[28].

$$b_0 \approx A_0^{1/2} \approx 8.4\times 10^{-8}\ \text{cm} \tag{36}$$

A more realistic estimation of $b_0$ may be obtained from the distance between adjacent molecular layers in the (110) direction which is parallel to the growth faces of the hexagonal single crystals of *i*-PS[41,42]. According to the unit cell given

**Table III.** Surface free energies and work for chain folding

| Polymer | Ref. | $T_m$ (°K) | Eq. | $\Delta H_f$ (joule/cm³) | $b_0$ (Å) | $A_0$ (Å²) | $K$ (deg) | $\sigma\cdot\sigma_e$ (erg²/cm⁴) | $\beta$ | $\sigma$ (erg/cm²) | $\sigma_e$ (erg/cm²) | $q$ (kcal/mol. fold) |
|---|---|---|---|---|---|---|---|---|---|---|---|---|
| *i*-PS | this | 515.2 | 30 | 91.1 | 8.4 | 70.5 | 232 | 87 | 0.083 | 6.35 | 13.7 | 2.9 |
| | work | 〃 | 〃 | 〃 | 5.5 | 〃 | 〃 | 133 | 0.083 | 4.16 | 32.0 | 6.5 |
| | 〃 | 〃 | 〃 | 〃 | 〃 | 〃 | 〃 | 〃 | 0.1 | 5.0 | 26.6 | 5.4 |
| | 7a | 513.0 | 28 | 86.0 | 8.4 | 〃 | 279 | 96 | 0.1 | 7.2 | 13.3 | 2.8 |
| PE | 10,36 | 416.2 | 28[a] | 280 | 4.11 | 18.3 | 230 | 540 | 0.083 | 9.6 | 56.0 | 2.9 |
| PCTFE | 27,36 | 494.2 | 28[a] | 91.1 | 5.6 | 36.4 | 280 | 156 | 0.083 | 4.2 | 37.0 | 3.9 |
| PB-1[b] | 37 | 403.2 | 28[a] | 96.2 | 7.45 | 55.5 | 290 | 128 | 0.1 | 7.2 | 17.8 | 2.8 |
| | 38 | 〃 | 〃 | 〃 | 〃 | 〃 | 305 | 135 | 〃 | 〃 | 18.7 | 3.0 |
| | 〃 | 〃 | 〃 | 〃 | 〃 | 〃 | 〃 | 〃 | 0.083 | 5.9 | 22.7 | 3.6 |
| POE[c] | 14 | 343.2 | 28[a] | 230[d] | 4.65 | 21.7 | 110 | 188 | 0.1 | 10.7 | 17.6 | 1.1 |
| 〃 | 〃 | 〃 | 〃 | 〃 | 〃 | 〃 | 〃 | 〃 | 0.083 | 8.9 | 21.1 | 1.3 |

[a] With universal WLF constants: $B = 2082$ deg, $T_g - T_\infty = 51.6$°C

[b] Form II

[c] $M_w \approx 8.10^5$

[d] In ref. 14, $\Delta H_f$ was assumed 280 joule·cm$^{-3}$.

by Natta *et al.*[40] the repeat distance of the (110) lattice planes is 11.0 Å units at 160°C. This distance corresponds to the separation of every second molecular layer, since the *i*-PS chains have alternatively left and right handed conformation in the consecutive layers parallel to the (110) direction[40]. Thus, the average separation of two adjacent layers normal to the growth faces may be evaluated as half of the repeat distance between the (110) planes, *i.e.*

$$b_0 = 5.5 \times 10^{-8} \text{ cm} \qquad (37)$$

The alternation of left and right handed helices in the consecutive layers may result in a rather severe segregation process near the growing face which should decrease appreciably the rate of growth.

In Table III we have listed the values of $\sigma\cdot\sigma_e$ derived from the best values of $K$, obtained from the third estimation of $\Delta f_v$, associated with the Vogel equation, (Eq. 30)*, while assuming for $b_0$ the two values given above (Eqs. 36 and 37). Table III in ludesalso the best estimation of Boon *et al.*[7a] based on slightly different input data (cf. ref. 43 and Table II).

By assuming two extreme values of $\beta$ (Eq. 34) equal to 0.083 or 0.1, obtained by Hoffman *et al.*[10,36] for PE and PCTFE, one can also evaluate the magnitude of the two surface free energies involved and the work for chain folding (Eq. 33). One can see that for *i*-PS the values of $\sigma_e$ and $q$ are rather sensitive to the magnitude of $b_0$ (Eqs. 36 and 37). This is due to the relatively large separation of the chains in the fold planes (parallel to the (110) direction) as compared to the distance $b_0$ (Eq. 37) between consecutive growth layers.

For comparative purposes Table III also shows the values of the nucleation parameters and the input data for some other polymers. In many respects ($T_m$, $\Delta H_f$, $b_0$, $K$, thus $\sigma$ and $\sigma_e$), *i*-PS has rather similar characteristics to that of PCTFE. In fact their spherulites grow more slowly than those of the other polymers listed, although at the same supercooling PCTFE grows[27] about 100 times faster than *i*-PS. This may be related to the different cross section of these two chains, which results in a substantially larger value of $q$ for *i*-PS than for PCTFE.

On the other hand PE and polyoxyethylene (PEO) have similar values of $\Delta H_f$, $b_0$ and $A_0$, thus of $\sigma$. However, the $K$ value of PEO seems abnormally low as compared to the other systems, which results in rather small values of $\sigma_e$ and $q$.

Although the overall growth rate at the same relative supercooling is controlled essentially by the value of $G_0$ (Eq. 1), the case by which polymer chains build up their crystalline phase near their

* As shown in Table II, Eq. 28 leads practically to the same value of $K$ as Eq. 30.

melting point seems to be correlated also to the work for chain folding, the values of which are increasing from PEO to *i*-PS. In this respect the theoretical treatment of surface nucleation of chain folded polymers leads to self-consistent results. However, the values of the nucleation parameters listed in Table III should be further substantiated by other independent investigations.

(c) In contrast to $K$, the second nucleation parameter $G_0$ varies in a rather large range depending both on the type of approach used for the evaluation of the transport term and on the magnitude of the parameters involved as shown in Table II. Its "best" value ($2.1\times10^{-2}$ cm·sec$^{-1}$) obtained from Eq. 30, is much smaller than the theoretical limit[10]: $b_0kT^*/h$ ($(5\sim8)\times10^5$ cm sec$^{-1}$), $T^*$ being the temperature at which $G$ reaches its maximum (Figure 3) and $h$ the Planck constant. This means that the growth rate is limited rather critically by specific effects, such as chain conformation and stereoregularity, which were not taken into account in the theoretical treatment (Eqs. 1 and 2). The rather large variations of $G_0$ from one sample to another as shown in Figure 7 for *i*-PS (or in Figure 4 in ref. 38 for PB-1), while using the same transport parameters, illustrate these effects directly. They are particularly important for blends[2] or "copolymers" built up by juxtaposing isotactic and atactic chain segments of the same monomer unit.

Consequently the comparison of the magnitude of $G_0$ for different polymeric systems seems somewhat hazardous, even by using the same type of approach for evaluating the transport term. Therefore, the "universality" of the value of $G_0$ as reported by Mandelkern *et al.*[4] can hardly be accepted. Since $G_0$ remains the most poorly defined parameter in the actual theories, clearly further work is needed to relate it explicitly to the molecular parameters, such as chain length, conformation tacticity *etc.*..., which may effect drastically the nucleation rate.

## CONCLUSIONS

From the above analysis of spherulitic growth rate of *i*-PS, the following conclusions may be drawn:

(a) If the experimental data cover a wide range of temperature, the theoretical expression of surface nucleation as modified by Hoffman et al. for polymeric systems may be successfully applied provided that the transport term is estimated according to the free volume concept (or a mathematically equivalent WLF or Vogel equation).

(b) The Adam-Gibbs theory leads to a much poorer fit of the data, except if the limiting temperature $T_2$ is considered as adjustable rather than being determined from direct investigations of the thermal properties of the material. In the former case the free volume and the configurational free energy approaches are practically equivalent, both involving two adjustable parameters for the transport term.

(c) The values of these are of reasonable magnitude in terms of the free volume concept and may be compared to those derived from the temperature dependence of the viscoelastic parameters or from other processes involving configurational mobility. More particularly, the limiting temperature $T_\infty$ at which the mobility approaches to zero seems to be almost independent of the type of investigation, provided that the data are analysed consistently.

However, for the growth process one has to account for the volume shrinkage due to the crystallization which contributes to the temperature coefficient of the local free volume near the growing face about as much as the brownian motion in the liquid phase.

(d) On the other hand, the magnitude of the free volume parameters is rather insensitive to the accuracy of the estimation of the free energy difference $\Delta f_v$ between the supercooled liquid and the crystal. However, by using the Adam-Gibbs approach for the evaluation of the transport term, the different approximations of $\Delta f_v$ may affect considerably this latter, since the transport and the nucleation terms are related through the excess configurational free energy, $T\cdot S_c$, of the liquid phase. In particular, the contribution of the transpot term depends critically on the limiting temperature $T_2$ where $S_c$ vanishes, the value of which is determined by the approximation used for estimating $\Delta f_v$.

(e) The nucleation parameter $K$ related to the free energy of the lateral and the fold surface and to the heat of fusion does not depend critically either on the approach used for the transport term or on the approximation of $\Delta f_v$. This conclusion is valid not only in the low temperature range

where the transport process is the main rate controlling factor, but also near the melting point at which the different evaluations of $\Delta f_v$ merge. (However, if the investigations are limited in a narrow temperature interval just below the melting point, the value of $T_m$ affects the magnitude of the nucleation parameters rather critically).

(f) The value of the nucleation parameter $K$ appears to be a characteristic constant of the material although its magnitude which may be related to the work for chain folding seems rather insensitive to the chemical composition of the polymer. Closer inspection shows however, that this work, related to the packing density and the stiffness of the chains, affects also the growth rate.

(g) Finally, the value of preexponential factor $G_0$ depends critically in the type of approximation used for estimating the transport term, and on the magnitude of the parameters involved. Undoubtedly this factor is affected by both processes controlling the growth rate and its magnitude seems to be the most specific for polymeric systems, related not only to their chemical composition, but also to their molecular conformation and stereospecificity.

Further progress, both theoretical and experimental, is needed to specify the contributions of these molecular parameters to the growth process of chain folded polymer crystals.

*Acknowledgement.* The authors are much indebted to Dr. J. J. André for compiling the computer program, and to Miss D. Levy and Mr. Ryuji Suzuki for their help in the above calculations.

## APPENDIX

One can write Eq. 26 as

$$Y = \log G + (B/2.303)(T - T_\infty)^{-1} = PX + Q \quad \text{(A1)}$$

with

$$\left.\begin{aligned} P &= K/2.303 \\ Q &= \log G_0 \end{aligned}\right\} \quad \text{(A2)}$$

and

$$X = \frac{\Delta H_f}{\Delta f_v \cdot T} = F(T) \quad \text{(A3)}$$

in which $\Delta f_v$ may be substituted by one of its approximate expressions (Eqs. 3, 15, and 19). The standard error on $K$ (or on Log $G_0$) may then be defined by

$$\sigma(K) = \sigma\left(\frac{N}{\Delta}\right)^{1/2} \quad \text{(A4)}$$

where

$$\sigma = \left[\frac{\sum (Y_i - PX_i - Q)^2}{N-2}\right]^{1/2} \quad \text{(A5)}$$

and

$$\Delta = N \sum X_i^2 - \left(\sum X_i\right)^2 \quad \text{(A6)}$$

$N$ being the number of experimental points, and $X_i$ and $Y_i$ the values calculated from Eqs. A 1 and A 3 by substituting the measured values of $G$ and $T$, and the trial values of $B$, (or $T_\infty$) letting $T_\infty$ (or $B$) vary.

## REFERENCES

1. A. S. Kenyon, R. C. Gross, and A. L. Wurstner, *J. Polym. Sci.*, **40**, 159 (1959).
2. H. D. Keith and F. J. Padden Jr., *J. Appl. Phys.*, **35**, 1270 and 1286 (1964).
3. J. N. Hay, *J. Polym. Sci.*, Part A, **3**, 433, 1965.
4. L. Mandelkern, N. L. Jain, and H. Kim, *J. Polym. Sci.*, Part A-2, **6**, 165 (1968)
5. H. Kim and L. Mandelekern, *J. Polym. Sci.*, A-2, **6**, 695 (1968).
6. J. Boon, a) *Thesis*, Delft, 1966, and b) *F. Polym. Sci.*, Part C, No. 16, 1739 (1967).
7. J. Boon, G. Challa and D. W. Van Krevelen, a) J. Polymer Sci., Part A-2, **6**, 1791 (1968, b) *J. Polym. Sci.*, A-2, **6**, 1835 (1968).
8. M. L. Williams, R. F. Landel, and J. D. Ferry, *J. Amer. Chem. Soc.*, **77**, 3701 (1955).
9. J. D. Hoffman, *J. Chem. Phys.*, **29**, 1192 (1958).
10. J. D. Hoffman, *S.P.E. Trans.*, **4**, 315 (1964).
11. J. H. Hagill, a) *J. Polym. Sci.*, Part A, **3**, 1195 (1965). b) Polymer, **6**, 367 (1965).
12. J. H. Magill and D. J. Plazek, *J. Chem. Phys.*, **46**, 3757 (1967).
13. D. J. Plazek and J. H. Magill, *J. Chem. Phys.*, **45**, 3038 (1966).
14. G. Vidotto, D. Levy, and A. J. Kovacs, *Kolloid Z. Z. Polym.* **230**, 289 (1969).
15. F. E. Karasz, H. E. Bair, and J. M. O'Reilly, *J. Phys. Chem.*, **69**, 2657 (1965).
16. T. Suzuki, D. Levy and A. J. Kovacs, to be published.
17. W. R. Krigbaum, D. R. Carpenter, and S. Newman, *J. Chem. Phys.* **62**, 1568 (1958).

18. G. Adam and J. H. Gibbs, *J. Chem. Phys.*, **43**, 1 (1965).
19. M. H. Cohen and D. Turnbull, *J. Chem. Phys.*, **31**, 1164 (1959).
20. D. Turnbull and J. C. Fisher, *J. Chem. Phys.*, **17**, 71 (1949).
21. J. I. Lauritzen and J. D. Hoffman, *J. Chem. Phys.*, **31**, 1680 (1959).
22. S. Glasstone, K. J. Laidler, and H. Eyring, "Theory of rate processes" Mc Graw-Hill Book-Co. New-York, (1941).
23. A. J. Kovacs, *Adv. Polym. Sci.*, **3**, 394 (1964).
24. G. C. Berry and T. G. Fox, *Adv. Polym. Sci.*, **5**, 261 (1967).
25. A. J. Kovacs, in "Relaxation Phenomena in Polymers". R. Longworth Ed. Interscience Publ., New-York, 1969 in press.
26. J. D. Hoffman and J. I. Lauritzen Jr., *J. Res. N.B.S.*, **65A**, 297 (1961).
27. J. D. Hoffman and J. J. Weeks, *J. Chem. Phys.*, **37**, 1723 (1962).
28. A. K. Doolittle, *J. Appl. Phys.*, **22**, 1471 (1951).
29. F. Danusso and G. Moraglio, *Rend. Accad. Naz. Lincei*, **27**, 381 (1958).
30. A. J. Kovacs, *Rheol. Acata*, **5**, 562 (1966).
31. H. Vogel, *Physik. Z.*, **22**, 645 (1921).
32. J. D. Ferry, "Viscoelastic Properties of Polymers" 2nd edition. Chap. 11. John Wiley & Sons. New-York, in press.
33. J. H. Magill, *J. Chem. Phys.*, **47**, 2802 (1967).
34. A. J. Kovacs, *J. Polym. Sci.*, **30**, 131 (1958).
35. R. Suzuki and A. J. Kovacs, paper presented at the Microsymposium on Rheology, Prague 1969, to be published.
36. F. Gornick and J. D. Hoffman, *Ind. Eng. Chem.*, **58**, 41 (1966).
37. J. Powers, J. D. Hoffman, J. J. Weeks, and F. A. Quinn, *J. Res. N.B.S.*, **A69**, 335 (1965).
38. G. Vidotto and A. J. Kovacs: *Kolloid Z., Z. Polym.*, **220**, 1 (1967).
39. D. J. Plazek, *J. Chem. Phys.* **69**, 3480 (1965).
40. G. Natta, P. Corradini, and I. W. Bassi, *Nuovo Cimento* (*Suppl. 15*), **1**, 68 (1960).
41. D. H. Keith, *J. Polym. Scl.*, Part A, **2**, 4339 (1964); and private communication.
42. J. Wittmann and A. J. Kovacs, to be published.
43. R. Dedenwaerder and J. F. Oth, *J. Chem. Phys.*, **56**, 940 (1959).